

Comparison of an Energy-based and a Momentum-based Agglomeration Model within an Euler-Lagrange LES Approach

N. Almohammed and M. Breuer

Department of Fluid Mechanics
Helmut-Schmidt University Hamburg

naser.almohammed@hsu-hh.de

breuer@hsu-hh.de

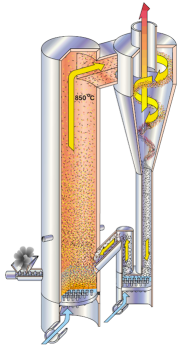
14th Workshop on Two-Phase Flow Predictions

- 1 **Introduction**
- 2 **Numerical Methodology**
 - Continuous Phase
 - Dispersed Phase
- 3 **Modeling of Particle Agglomeration**
 - Momentum-based Agglomeration Model
 - Energy-based Agglomeration Model
- 4 **Model Validation**
 - Shear flow
 - Turbulent Channel Flow
- 5 **Conclusions and Outlook**

- 1 Introduction**
- 2 Numerical Methodology**
 - Continuous Phase
 - Dispersed Phase
- 3 Modeling of Particle Agglomeration**
 - Momentum-based Agglomeration Model
 - Energy-based Agglomeration Model
- 4 Model Validation**
 - Shear flow
 - Turbulent Channel Flow
- 5 Conclusions and Outlook**

Turbulent Particle-Laden Flows

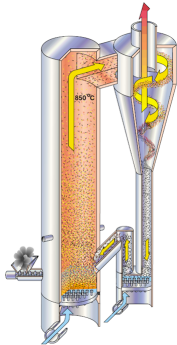
- Industrial applications
- Medical technology
- Natural phenomena



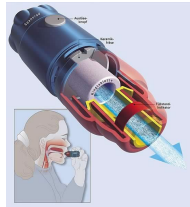
Fluidized bed

Turbulent Particle-Laden Flows

- Industrial applications
- **Medical technology**
- Natural phenomena



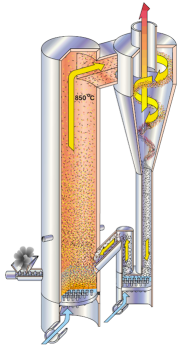
Fluidized bed



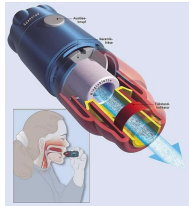
Inhalation spray

Turbulent Particle-Laden Flows

- Industrial applications
- Medical technology
- **Natural phenomena**



Fluidized bed



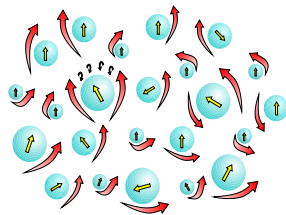
Inhalation spray



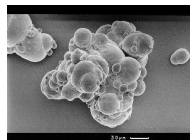
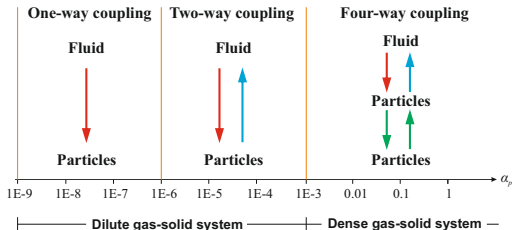
Dust storm

Complex Flow Dynamics

- Gas-particle interaction
- Particle-gas interaction (feedback)
- Particle-particle collision
- Agglomeration of cohesive particles



Turbulent particle-laden flow

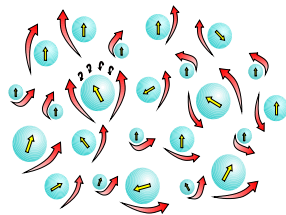


Real agglomerate

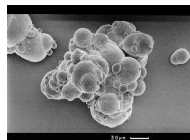
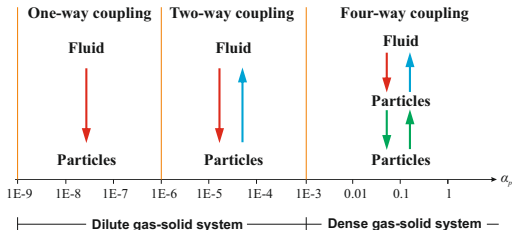
(Sommerfeld, MVT Website)

Complex Flow Dynamics

- Gas-particle interaction
- Particle-gas interaction (feedback)
- Particle-particle collision
- Agglomeration of cohesive particles



Turbulent particle-laden flow

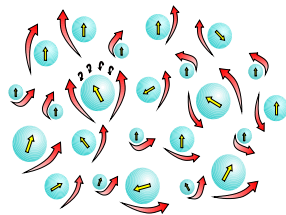


Real agglomerate

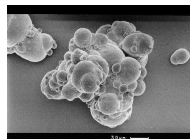
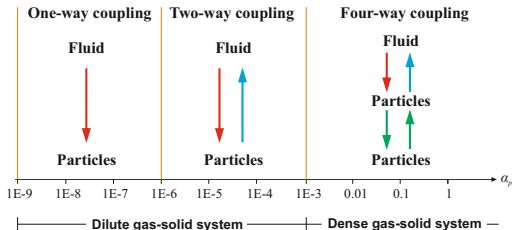
(Sommerfeld, MVT Website)

Complex Flow Dynamics

- Gas-particle interaction
- Particle-gas interaction (feedback)
- **Particle-particle collision**
- Agglomeration of cohesive particles



Turbulent particle-laden flow

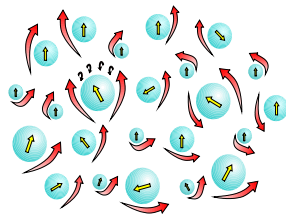


Real agglomerate

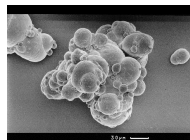
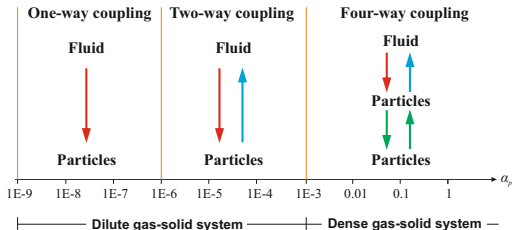
(Sommerfeld, MVT Website)

Complex Flow Dynamics

- Gas-particle interaction
- Particle-gas interaction (feedback)
- Particle-particle collision
- **Agglomeration of cohesive particles**



Turbulent particle-laden flow



Real agglomerate

(Sommerfeld, MVT Website)

Motivation

- Relevance of turbulent particle-laden flows to processes employed in a wide range of applications
- Advanced understanding of the complex flow behavior in the context of particle dispersion and agglomeration
- Flexibility and cheapness of the numerical simulations in comparison with experiments
- Advanced predictive technique for describing fluid motion, Large-Eddy Simulation, coupled with a deterministic collision model
- Extension of our in-house code *LESOC* to include particle agglomeration

Objectives

- **Modeling**
 - Particle agglomeration
 - Kinetics of the resulting agglomerate
 - Structure of the agglomerate
- **Implementation**
 - CFD-code *LES OCC*
 - Testing based on simple test cases
- **Validation**
 - Laminar shear flow
 - Turbulent channel flow

- 1 Introduction
- 2 **Numerical Methodology**
 - Continuous Phase
 - Dispersed Phase
- 3 **Modeling of Particle Agglomeration**
 - Momentum-based Agglomeration Model
 - Energy-based Agglomeration Model
- 4 **Model Validation**
 - Shear flow
 - Turbulent Channel Flow
- 5 **Conclusions and Outlook**

CONTINUOUS PHASE

- **LESOCC** (Large Eddy Simulation On Curvilinear Coordinates)
- **Navier–Stokes solver** (incompressible fluid)
- **3D Finite volume method**
 - ☞ Curvilinear body–fitted coordinate system
 - ☞ Non–staggered (cell–centered) grid arrangement
 - ☞ Block–structured grids
- **Spatial discretization**
 - ☞ Viscous fluxes: central differences $O(\Delta x^2)$
 - ☞ Convective fluxes: five different schemes, central diff. $O(\Delta x^2)$
- **Temporal discretization**
 - ☞ Predictor step (momentum eqns.): low–storage Runge–Kutta scheme, $O(\Delta t^2)$
 - ☞ Corrector step (pressure–correction equation): SIP solver (ILU)
- **Pressure–velocity coupling:** Momentum interpolation of Rhie & Chow
- **Various subgrid-scale and wall models**
- **High–performance computing techniques:** Vectorized & parallelized

DISPERSED PHASE

Dispersed Phase

- **Modeling assumptions**

- Lagrangian frame of reference for the dispersed phase
- High density ratio $\rho_p/\rho_f \gg 1$
- Drag, gravity, buoyancy and lift forces
- High volume fraction: Two- and four-way coupling

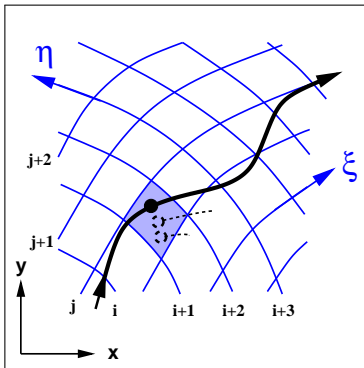
- **Newton's second law**

- $$\frac{d\mathbf{u}_p}{dt} = \frac{\mathbf{u}_f - \mathbf{u}_p}{\tau_p/\alpha} + \mathbf{g} \left(1 - \frac{\rho_f}{\rho_p} \right) + \frac{F_L}{m_p}$$

- $$\frac{d\boldsymbol{\omega}_p}{dt} = -\frac{10}{3\tau_p} \boldsymbol{\Omega}_{rel} \quad \text{with} \quad \boldsymbol{\Omega}_{rel} = \frac{1}{2} \nabla \times \mathbf{u}_f - \boldsymbol{\omega}_p$$

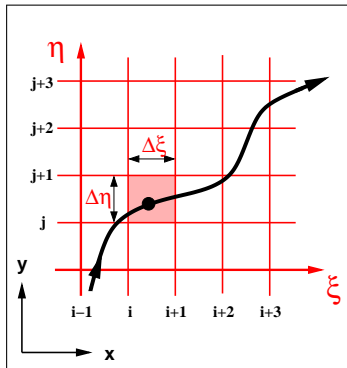
- $$\frac{d\mathbf{x}_p}{dt} = \mathbf{u}_p$$

Physical Space



- Curvilinear grid
- Point location not trivial
- Time-consuming local and global search algorithms

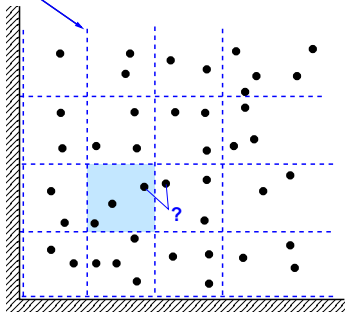
Computational Space



- Orthonormal grid
- Point location trivial
- No search of particle's new position required

Particle-Particle Collision Detection

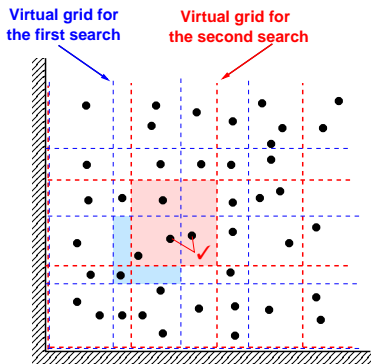
Virtual grid for
the first search



Likely collision partners in virtual cells

(First Search)

Particle-Particle Collision Detection



Likely collision partners in virtual cells
(Second Search)

- Only particles in a virtual cell are checked for collisions
- Second search to find closest particles in neighboring cells
- Reduction of computational effort from $\mathcal{O}(N_p^2)$ to $\mathcal{O}(N_p)$

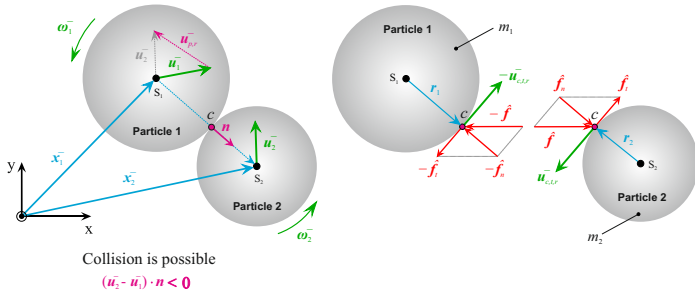
Hard-Sphere Model

- Spherical rigid particles
- Particle deformation neglected
- Friction obeys Coulomb's law

Hard-Sphere Model

- Spherical rigid particles
- Particle deformation neglected
- Friction obeys Coulomb's law

Particle-Particle Collision



- 1 Introduction
- 2 Numerical Methodology
 - Continuous Phase
 - Dispersed Phase
- 3 Modeling of Particle Agglomeration
 - Momentum-based Agglomeration Model
 - Energy-based Agglomeration Model
- 4 Model Validation
 - Shear flow
 - Turbulent Channel Flow
- 5 Conclusions and Outlook

Particle Agglomeration

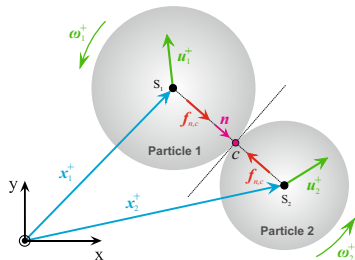
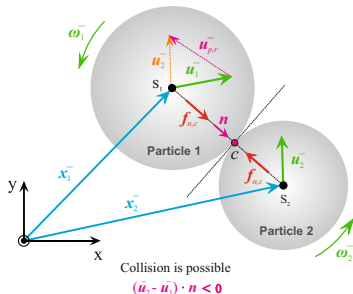
- **Modeling assumptions**
 - Hard-sphere model
 - Dry, electrostatically neutral particles
 - Van-der-Waals force
 - Spherical agglomerates
- **Agglomeration models**
 - Momentum-based agglomeration model
 - Energy-based agglomeration model

**MOMENTUM-BASED
AGGLOMERATION MODEL
(MAM)**

Momentum-based Agglomeration Model [1]

Normal component of the total impulse

$$\hat{f}_n = \underbrace{\hat{f}_{n,a}}_{\text{Repulsive Impulse}} + \underbrace{\hat{f}_{n,c}}_{\text{Cohesive Impulse}}$$



[1] Breuer, M., Almomammed, N.: *Modeling and simulation of particle agglomeration in turbulent flows using a hard-sphere model with deterministic collision detection and enhanced structure models*, Int. J. of Multiphase Flow 73, 171–206, (2015).

Collision Type

- **No-slip condition**

$$|\mathbf{u}_{c,t}^-| \leq \frac{7}{2} \frac{\mu_{st,w}}{1 + e_{t,w}} (\hat{f}_{n,a} + \hat{f}_{n,c})$$

→ Cohesive impulse enhances the friction at the contact point

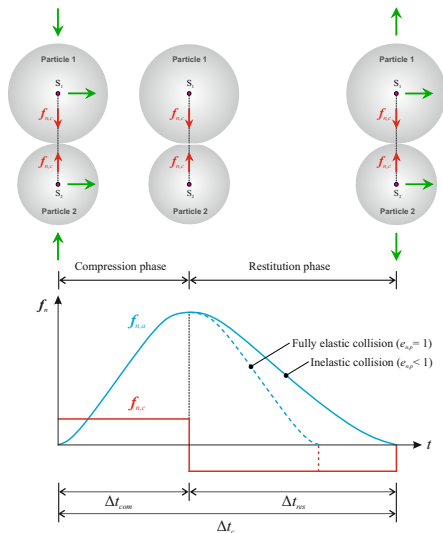
- **Sticking collision**

Collision partners stick to each other

- **Sliding collision**

Collision partners slide over each other

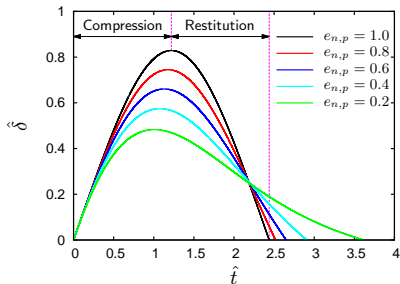
Modeling of the Cohesive impulse



$$\hat{f}_{n,c}^* = \underbrace{\frac{1}{\hat{m}} \int f_{n,c} dt}_{\text{Compression}} + \underbrace{\frac{1}{\hat{m}} \int f_{n,c} dt}_{\text{Restitution}}$$

$$\hat{f}_{n,c}^* = -\frac{1}{\hat{m}} f_{n,c} \Delta t_c^*$$

with: $\Delta t_c^* = \Delta t_{res} - \Delta t_{com}$



Agglomeration Conditions [1]

- **Limiting impulse**

$$\hat{f}_{l,n} = \hat{f}_l \cdot \mathbf{n} = -(\mathbf{u}_2^- - \mathbf{u}_1^-) \cdot \mathbf{n}$$

$$\hat{f}_{l,t} = \hat{f}_l \cdot \mathbf{t} = -(\mathbf{u}_2^- - \mathbf{u}_1^-) \cdot \mathbf{t}$$

- **Sticking collision** → One condition

$$\hat{f}_{l,n} > \hat{f}_{n,a} + \hat{f}_{n,c}^* \Rightarrow -\hat{f}_{n,c}^* > -e_{n,p} (\mathbf{u}_2^- - \mathbf{u}_1^-) \cdot \mathbf{n}$$

- **Sliding collision** → Two conditions

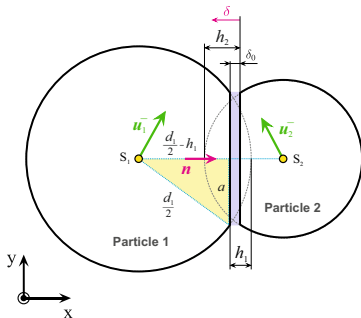
$$\hat{f}_{l,n} > \hat{f}_{n,a} + \hat{f}_{n,c}^* \quad \& \quad |\hat{f}_{l,t}| < |\hat{f}_t|$$

$|\hat{f}_t|$ has to be large enough to stop the particle from further sliding.

**ENERGY-BASED
AGGLOMERATION MODEL
(EAM)**

Energy-based Agglomeration Model [2]

- First proposed by Hiller (1981)
- Applied by Sommerfeld and Ho (2002), Ho (2004)
 - Head-on frictionless collision
 - $\Delta E_{vdW} \geq E_{kin,r}^+$
- Extended by Alletto (2014)
 - Inclusion of rotation and friction
 - $\Delta E_{vdW} \geq E_{kin,r}^+ + E_{rot}^+ - E_{rot,ag}$
 - Rebound in either the normal or the tangential direction
- Improved by Almohammed and Breuer [2]



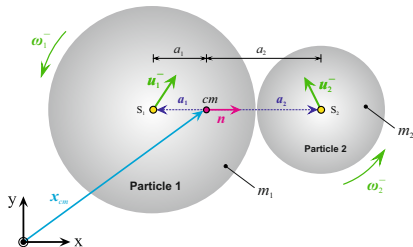
[2] Almohammed, N., Breuer, M.: *Modeling and simulation of agglomeration in turbulent particle-laden flows: A comparison between energy-based and momentum-based agglomeration models*, Powder Technology, submitted, (2015).

Kinetics of an Agglomerate [1]

- **Position and velocity**

$$\mathbf{x}_{ag}^+ = \frac{m_1 \mathbf{x}_1^- + m_2 \mathbf{x}_2^-}{m_1 + m_2}$$

$$\mathbf{u}_{ag}^+ = \frac{m_1 \mathbf{u}_1^- + m_2 \mathbf{u}_2^-}{m_1 + m_2}$$



- **Angular momentum**

$$\mathbf{L}_{ag} = I_1 \boldsymbol{\omega}_1^- + I_2 \boldsymbol{\omega}_2^- + \frac{\hat{m}}{2} (d_1 + d_2) \mathbf{n} \times (\mathbf{u}_2^- - \mathbf{u}_1^-)$$

- **Angular velocity**

$$\mathbf{L}_{ag} = [I_{ag}] \boldsymbol{\omega}_{ag} \quad ; \quad [I_{ag}] = \begin{pmatrix} I_{xx} & I_{xy} & I_{xz} \\ I_{yx} & I_{yy} & I_{yz} \\ I_{zx} & I_{zy} & I_{zz} \end{pmatrix}$$

Agglomerate Structure Models [1]

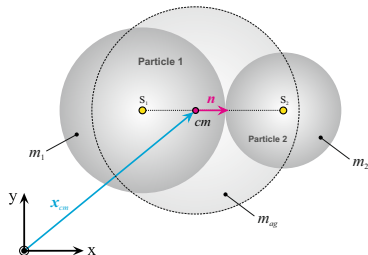
- 1 **Volume-equivalent Sphere Model (VSM)**
- 2 Inertia-equivalent Sphere Model (ISM)
- 3 Closely-packed Sphere Model (CSM)

$$\omega_{ag} = \frac{L_{ag}}{I_{ag}}$$

$$I_{ag} = \frac{1}{10} m_{ag} d_{ag}^2$$

$$m_{ag} = m_1 + m_2$$

$$d_{ag} = \sqrt[3]{d_1^3 + d_2^3}$$



Structure Models [1]

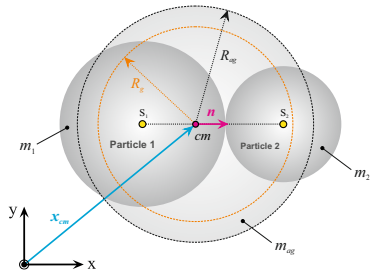
- 1 Volume-equivalent Sphere Model (VSM)
- 2 **Inertia-equivalent Sphere Model (ISM)**
- 3 Closely-packed Sphere Model (CSM)

$$\omega_{ag} = \frac{L_{ag}}{I_{ag}} \quad ; \quad I_{ag} = \frac{1}{10} m_{ag} d_{ag}^2$$

$$\frac{2}{3} m_{ag} R_g^2 = \frac{2}{5} m_{ag} R_{ag}^2$$

$$d_{ag} = \sqrt{20/3} R_g \quad ;$$

$$\rho_{ag} = \frac{\rho_1 d_1^3 + \rho_2 d_2^3}{d_{ag}^3} \neq \rho_1$$



Structure Models [1]

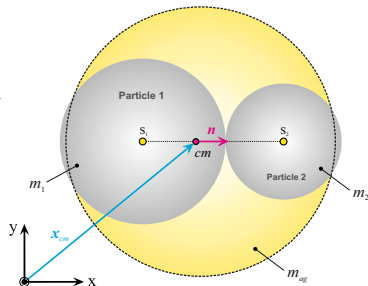
- 1 Volume-equivalent Sphere Model (VSM)
- 2 Inertia-equivalent Sphere Model (ISM)
- 3 Closely-packed Sphere Model (CSM)

$$\omega_{ag} = \frac{L_{ag}}{I_{ag}} \quad ; \quad I_{ag} = \frac{1}{10} m_{ag} d_{ag}^2$$

$$\rho_{ag} = f_{pack} \rho_o \quad \text{with: } 0 < f_{pack} < 1$$

$$f_{pack} = \frac{V_{sphere}}{V_{cube}}$$

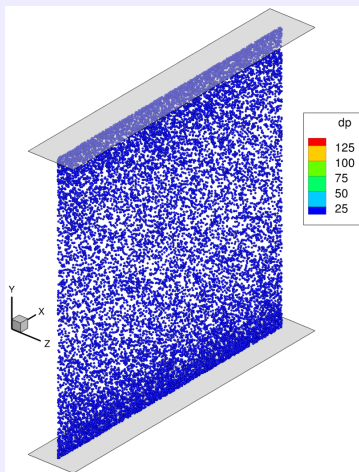
$$d_{ag} = \left(\frac{\rho_1 d_1^3 + \rho_2 d_2^3}{\rho_{ag}} \right)^{1/3}$$



- 1 Introduction
- 2 Numerical Methodology
 - Continuous Phase
 - Dispersed Phase
- 3 Modeling of Particle Agglomeration
 - Momentum-based Agglomeration Model
 - Energy-based Agglomeration Model
- 4 Model Validation
 - Shear flow
 - Turbulent Channel Flow
- 5 Conclusions and Outlook

2D Lamellar Shear Flow [3]

- Constant shear rate
 $\dot{\gamma} = 71 \text{ s}^{-1}$
- $2\delta \times 2\delta \times \delta$ ($\delta = 0.0195 \text{ m}$)
- $64 \times 64 \times 10$ grid points
- Periodic boundary conditions in x - and z -direction
- No-slip condition on the wall
- 20,140 primary particles with $d_p = 25 \mu\text{m}$



[3] Balakin, B., Kosinski, P., Hoffmann, A. C.: *The collision efficiency in a shear flow*, Chemical Engineering Science **68**, 305–312, (2012).

Zeroth Moment of Particle Size Distribution

$$M_0(t) = \frac{M_0(0)}{1 + 0.5 \beta K M_0(t) t}$$

1 Theoretical Model

2 Numerical Results

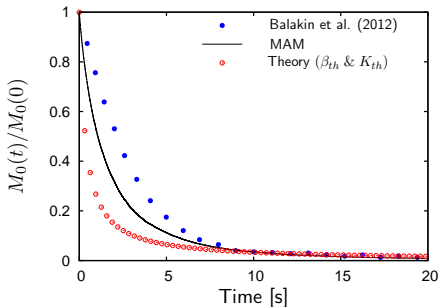
• Agglomeration rate

$$\beta = \beta_{th}^* = f(\bar{\lambda}) \left(\frac{8H}{36\pi\mu\dot{\gamma}d_0^3} \right)^{0.18}$$

• Collision frequency

$$K^{**} = \frac{\dot{\gamma}}{\pi} \left(V_1^{1/3} + V_2^{1/3} \right)^3$$

$$K_{th} = 4/3 \dot{\gamma} (d_0)^3$$



(van de Ven and Mason, 1977)*

(Saffman and Turner, 1956)**

Zeroth Moment of Particle Size Distribution

$$M_0(t) = \frac{M_0(0)}{1 + 0.5 \beta K M_0(t) t}$$

1 Theoretical Model

2 Numerical Results

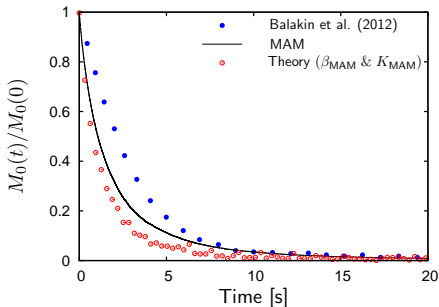
• Agglomeration rate

$$\beta = \beta_{\text{MAM}}$$

• Collision frequency

$$K^{**} = \frac{\dot{\gamma}}{\pi} \left(V_1^{1/3} + V_2^{1/3} \right)^3$$

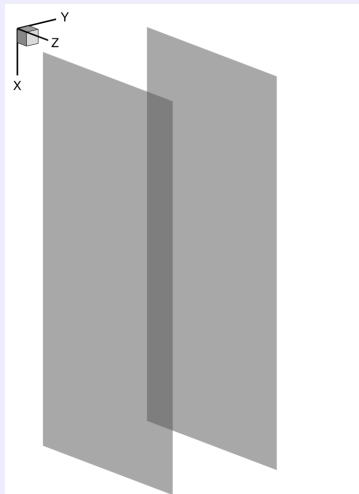
$$K_{\text{MAM}} = \frac{\dot{\gamma}}{\pi N_{\text{col}}} \sum_{i=1}^{N_{\text{col}}} \left(V_{1,i}^{1/3} + V_{2,i}^{1/3} \right)^3$$



(Saffman and Turner, 1956) **

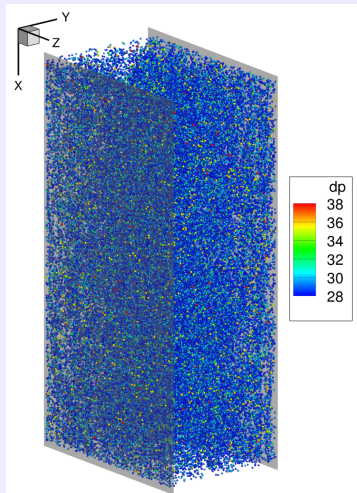
3D Turbulent Channel Flow [1,2]

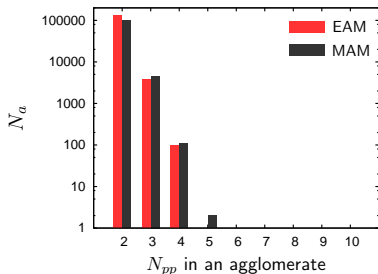
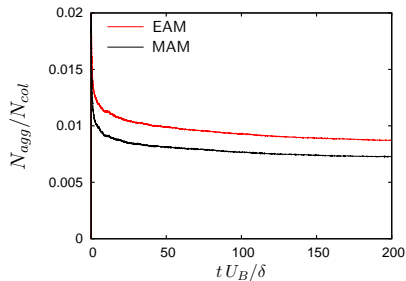
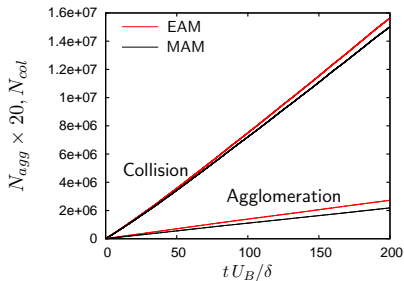
- $Re = 11,900$ ($Re_\tau = 644$)
- $2\pi\delta \times 2\delta \times \pi\delta$ ($\delta = 0.02$ m)
- $128 \times 128 \times 128$ grid points
- Periodic boundary conditions in x - and z -direction
- No-slip condition on the wall
- 6×10^6 primary particles with $d_p = 4$ and $12 \mu\text{m}$
- Elastic particle-particle and particle-wall collisions with friction
- Smooth and rough walls



3D Turbulent Channel Flow [1,2]

- $Re = 11,900$ ($Re_\tau = 644$)
- $2\pi\delta \times 2\delta \times \pi\delta$ ($\delta = 0.02$ m)
- $128 \times 128 \times 128$ grid points
- Periodic boundary conditions in x - and z -direction
- No-slip condition on the wall
- 6×10^6 primary particles with $d_p = 4$ and $12 \mu\text{m}$
- Elastic particle-particle and particle-wall collisions with friction
- Smooth and rough walls





In comparison with MAM, EAM predicts:

- Higher N_{col} and N_{agg}
- Higher agglomeration rate
- Greater N_a of two-particle agglomerates

Submodels (SMs)

- **Two-way Coupling**

Feedback effect of the particles on the continuous phase

$$f_i^{PSIC} = - \sum_{k=1}^{N_p} \frac{F_{D,i}}{\Delta Vol} = - \sum_{k=1}^{N_p} \frac{3 \mu_f \pi d_p \alpha (u_{f,i} - u_{p,i})}{\Delta Vol}$$

- **Lift forces**

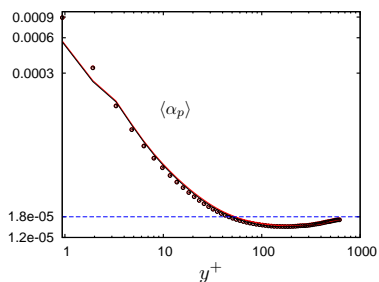
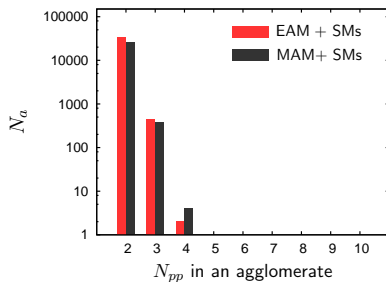
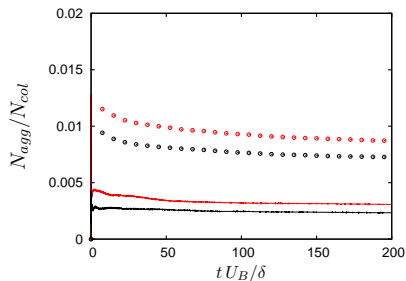
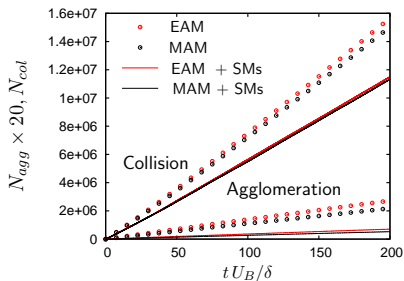
- Saffman force
- Magnus force

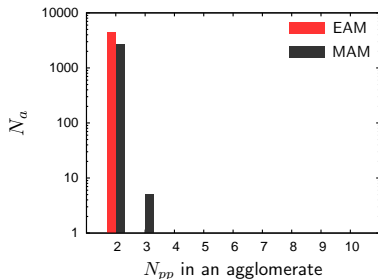
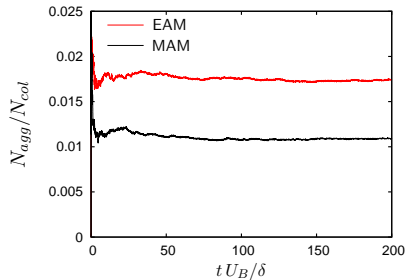
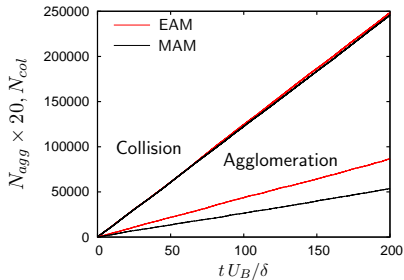
- **Subgrid-scale model for the particles**

Effect of the unresolved scales within LES on particle motion

$$\mathbf{u}_f = \bar{\mathbf{u}}_f + \mathbf{u}'_f \quad \text{with} \quad \mathbf{u}'_f = \sqrt{\frac{2}{3} k_{SGS}} \boldsymbol{\xi}$$

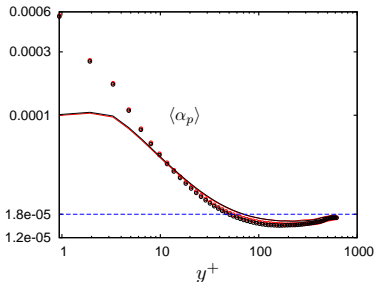
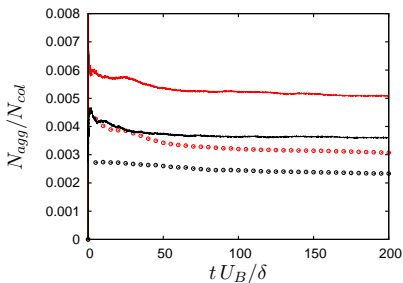
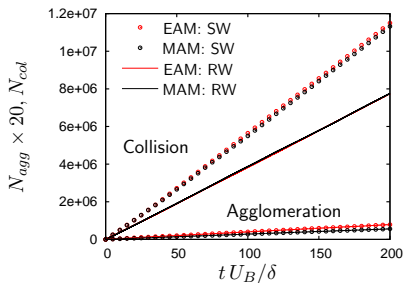
$$k_{SGS} = \frac{1}{2} (\bar{\mathbf{u}}_f - \bar{\bar{\mathbf{u}}}_f)^2$$





- Similar trends as for large particles
- Higher ΔE_{vdW} and cohesive impulse
- Higher agglomeration rate

Effect of the Diameter of Primary Particles



- Significant reduction of N_{col}
- Lower volume fraction in the near-wall region
- Higher agglomeration rate by EAM than MAM

- 1 **Introduction**
- 2 **Numerical Methodology**
 - Continuous Phase
 - Dispersed Phase
- 3 **Modeling of Particle Agglomeration**
 - Momentum-based Agglomeration Model
 - Energy-based Agglomeration Model
- 4 **Model Validation**
 - Shear flow
 - Turbulent Channel Flow
- 5 **Conclusions and Outlook**

Conclusion

- Improvement of two agglomeration models in the framework of a hard-sphere model
- Proposal of two structure models for an agglomerate
- Successful validation of the MAM in a shear flow
- Application of both agglomeration models in turbulent particle-laden channel flow
- Prediction of similar trends of the physical behavior of the agglomeration process by both agglomeration models
- MAM is superior to EAM due to accurate results and the reduced necessity of empirical parameters

Outlook

- Validation of the agglomeration models with experimental test cases (e.g., shear layer by Ho (2004))
- Comparison with other numerical test cases
- Investigation of the effect of deposition on the walls
- Inclusion of liquid bridge
- Investigation of the effect of deposition on the walls
- Break-up of particles or agglomerates

Thanks for your attention

Acknowledgments

Financially supported by the *Deutsche Forschungsgemeinschaft* (BR 1847/13-1)
All kinds of support are gratefully acknowledged.



Calculation Procedure [2]

- Collision without considering the van-der-Waals force
- Cohesive impulse introduced based on the van-der-Waals interaction

$$\hat{\mathbf{f}}_{ag} = \hat{\mathbf{f}}_{ag,n} + \hat{\mathbf{f}}_{ag,t}$$

Difference of the van-der-Waals energy

- $\Delta E_{\text{vdW}} = \frac{H}{12 \delta_0^2} d_1^2 d_2^2 |\mathbf{u}_2^- - \mathbf{u}_1^-| \left[\frac{\rho_1 \rho_2 (1 - e_{n,p}^2)}{6 \bar{p} (d_1 + d_2) (\rho_1 d_1^3 + \rho_2 d_2^3)} \right]^{\frac{1}{2}}$
- Maximum contact pressure \bar{p} may not be available in the literature.

Overlap in the normal direction

$$\frac{d^2 \hat{\delta}}{d\hat{t}^2} + 2\alpha \hat{\delta}^{1/4} \frac{d\hat{\delta}}{d\hat{t}} + \hat{\delta}^{3/2} = 0$$

$$\hat{t} = t \left(C^{-1/2} r^{1/2} K/m \right)^{1/2}$$

$$\hat{\delta} = C \delta / r$$

$$\text{with: } C = r \left(\frac{K}{m u_n^2} \right)^{2/5}$$

Cohesive impulse

$$\hat{f}_{n,c}^* = -0.196 \left\{ \frac{\hat{m}^{-3}}{\hat{E}^2 (\mathbf{u}_1^- - \mathbf{u}_2^-) \cdot \mathbf{n}} \right\}^{\frac{1}{5}} \frac{H}{\delta_0^2} \hat{r}^{\frac{4}{5}} \Delta \hat{t}_{dif}$$

